# Calculations on the arrival-time distribution and energy content of extensive air showers at large core distances



1968 J. Phys. A: Gen. Phys. 2 50

(http://iopscience.iop.org/0022-3689/2/1/008)

J. PHYS. A (GEN. PHYS.), 1969, SER. 2, VOL. 2. PRINTED IN GREAT BRITAIN

# Calculations on the arrival-time distribution and energy content of extensive air showers at large core distances

A. J. BAXTER
Department of Physics, University of Leeds†
*MS. received* 21*st May* 1968

**Abstract.** Particles comprising an extensive air shower do not originate from a point but are produced as secondaries to the products of interactions which take place along an axial core region. Their structure or arrival-time distribution should be related to their production depth and propagation properties.

A detailed Monte Carlo calculation has been made on the delays arising in the development of the electron–photon component to form a basis for the interpretation of experimental observations.

Results are presented for the estimated time-delay distributions in an extensive air shower of primary energy $9 \times 10^{16}$ ev at radial core distances of 200, 400 and 600 m. Also considered are the energy spectra of photons at such distances, the lateral distribution of energy in the front and the relative muon and electron–photon contributions.

## 1. Introduction

Information on the properties of large extensive air showers, as revealed by particle detectors, is determined by a sampling of the shower front at a few spatially separated points of limited area. In general, such measurements are necessarily made at large distances from the shower core, and certain assumptions concerning the nature of a shower have to be made before the parameters of a particular shower can be estimated.

One guide to shower development, provided sufficient resolution can be achieved, is the distribution in the time of arrival of the particles at the detector, or of the energy carried by them.

Early work on the arrival-time distribution, in small showers, such as that due to Bassi *et al.* (1953), indicated that the electron–photon component was confined to a thin disk of the order of 1–2 m thick, slightly in advance of a marginally thicker muon front. However, Linsley and Scarsi (1962), who give references to other earlier experiments, show that for much larger showers, of mean size $2 \times 10^7$, the front is considerably broadened at distances in excess of 200 m from the core. The recent calculations of Locci *et al.* (1967), whilst confirming the picture of Bassi *et al.* at core distances of the order of tens of metres, demonstrate the broadening of the front with distance.

The present paper reports a calculation on the propagation of the electron–photon component, which, when coupled with similar results on the muon component (Hillas 1966), has formed a basis for interpreting the experimentally observed arrival-time distribution (Baxter *et al.* 1967). These data were obtained using the Haverah Park 500 m array for showers of primary energy about $10^{17}$ ev, the same order as that of Linsley and Scarsi.

## 2. Calculation

The use of a digital computer allows the problem of the development of an electron–photon cascade to be solved by simulating the behaviour of individual particles using the Monte Carlo technique. This method can form a direct means of estimating the probable delay by path differences of particles in the cascade and can then be used to derive the shower-front structure.

In this work a series of such simulations for different primary electron or photon energies and heights of initiation is treated as a set of sub-showers which, when suitably weighted, will correspond effectively to the electron–photon situation in large extensive air showers.

† Now at Department of Physics, The University of Calgary, Calgary, Alberta, Canada.

The interactions involved—bremsstrahlung, pair production and Compton effect—were simulated by the methods developed by Butcher and Messel (1960). The cross sections required were taken from Rossi (1952). In the case of bremsstrahlung, the true cross section was replaced by a constant term for the radiation of photons below 0·5 MeV, to avoid the low-energy divergence. At any one instant in the calculation, the movement of just one particle was considered, characterized by the following seven parameters: the coordinates $x, y, z$ of the last point of interaction, the direction of motion in a $\theta$, $\phi$ coordinate system, the energy of the particle and, finally, the delay acquired by the particle with respect to a plane front propagating in the direction of a vertical shower axis at the relativistic limit.

The electron energies were modified in accordance with the ionization loss appropriate to each interval traversed, and the direction of motion was adjusted at each step to allow for scattering. After an interaction, the secondary electron or photon of higher energy was stored away and the particle of lower energy was followed through its further interactions, until it reached ground level, or until its energy had fallen below the lowest energy of interest. Each particle in the store was considered in turn, additional particles being stored where necessary until the complete development had been described. At each stage between interactions, distances in g cm$^{-2}$ were converted to metres by a function dependent on altitude to facilitate the assessment of the resultant delays.

The treatment of scattering used in the calculation was to take the purely Gaussian multiple-scattering distributions, as presented in Rossi (1952), but modified to include the large-angle 'single scattering' events (appendix 1). Although the number of effective single-scattering events is relatively small, it is just these which contribute most to the time distribution observed at large distances from the core.

The time-delay produced in any interval corresponds, for photons, just to the extra path length due to non-vertical propagation. For electrons a further, velocity-dependent, mean straggling term was included in the calculations, but it was found to be of secondary importance to the delays which arise, at large core distances, from the propagation of lower energy photons at large angles to the core.

Calculations were performed for primary energies of $10^3$, $3\times10^3$, $10^4$, $3\times10^4$ and $10^5$ MeV, at a series of injection altitudes in 80 g cm$^{-2}$ intervals. The number of simulations made at the different energies were 100, 100, 26, 16 and 9 respectively for both electron and photon initiation. The lowest secondary energy was taken as 4 MeV, but 10% of the injections were modified to assess contributions down to 0·6 MeV, the electron Čerenkov threshold of the detectors used by the Haverah Park array (Tennent 1967 b). To obtain the situation in an extensive air shower of primary energy $9\times10^{16}$ eV, these cascades were weighted by coefficients representing the injection of $\gamma$-rays by decaying $\pi^0$ mesons from a nuclear cascade model (Hillas 1966) for a primary proton.

For high energies the $\gamma$-ray production spectrum is given by

$$P(E)\,\mathrm{d}E = \frac{2\,\mathrm{d}E}{E_\pi}$$

where $E_\pi$ is the neutral pion energy.

Hence for an energy interval $j$, defined by $E_j = \exp(Aj)$, where $A$ is a constant, the number of photons $N_{ji}$ produced in an interval $i$ is given by

$$N_{ji} = \frac{2(1-C)^2C^{(j-i-1)}}{A} \qquad \text{when } i < j$$

and

$$N_{jj} = 2\left(1 - \frac{(1-C)}{A}\right) \qquad \text{when } i = j$$

where $C = \exp(-A)$.

For those cases where the photon energies were above the energies included in the Monte Carlo calculation, a calculation of the longitudinal electron–photon cascade under 'approximation A' was incorporated, to sub-divide the energy among secondary particles through the atmosphere. Once again, the electrons and photons produced below the selected limiting energy were filtered out at the appropriate altitude level.

## 3. Arrival-time distributions

The arrival-time distributions (calculated in the manner just described) of the energy of the electron–photon component in the shower front at core distances of 200, 400 and 600 m are shown in figure 1. Also indicated are the muon time-delay distributions given

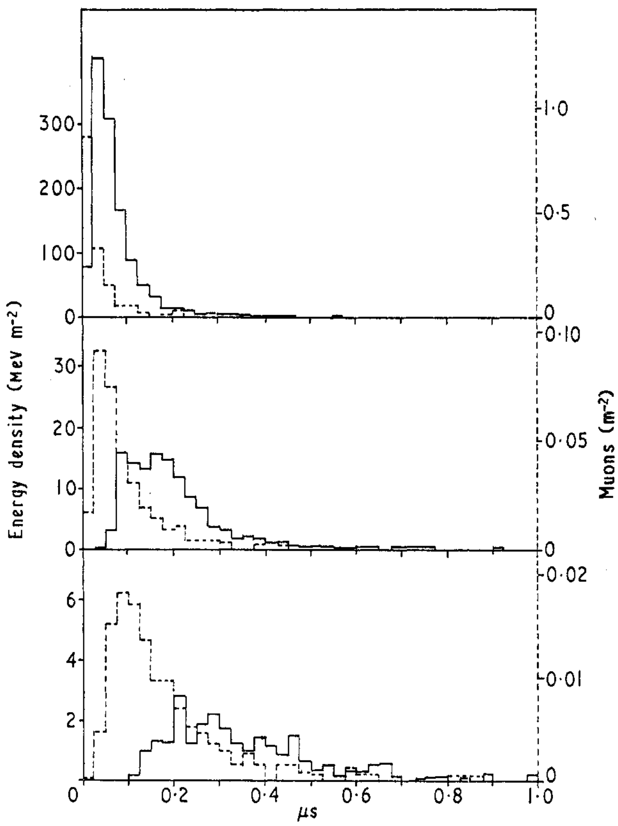


Figure 1. Arrival-time distributions of the energy in the electron–photon component at core distances of 200, 400 and 600 m. The broken lines indicate the estimated muon time-delay distributions (Hillas 1966).

by Hillas (1966). The latter were derived from a transformation of the contributary muon energy–altitude production spectra, taking into account, in addition to geometrical delays, delays due to velocity differences, geomagnetic and Coulomb scattering which are only important at the lower energies and can be described by a first-order approximation. The area under these distributions, the total electron–photon component energy density and muon particle density are normalized in proportion to the predicted responses in the Haverah Park water Čerenkov detectors as indicated in table 1.

These time arrival distributions have proved useful in interpreting the experimental results (Baxter *et al.* 1967) derived by a method of pulse analysis (Baxter *et al.* 1966).

**Table 1. Variation with core distance of the muon to total muon plus electron–photon Čerenkov response ratio in the Haverah Park detectors**

| Core distance (m) | 200 | 400 | 600 |
|---|---|---|---|
| $\mu/(\mu+e)$ calc. | 0·31 | 0·52 | 0·66 |
| $\mu/(\mu+e)$ expt. | 0·32 | 0·54 | 0·73 |

Since only limited areas of detector can be employed in the experimental work, the number of particles detected in the peripheral regions of a shower is comparatively small. To relate the above distributions to what may be observed in an actual shower, random sampling methods have been employed as indicated in appendix 2.

There is a considerable likelihood, especially at large core distances, for a variation of the time of arrival of the first signal detected. This first signal is most likely to be muonic in origin, since that component arrives substantially before the electron–photon component, and an isolated early photon (because of its small energy) might not be resolved in a deep detector. Since the arrival times of the first signal at a number of separated detectors is used to estimate the arrival direction of the shower, an inherent spread in estimated arrival direction thus arises, even neglecting measurement error. This error is related to the spacing and area of the detectors used in the sampling. For an array such as the 500 m Haverah Park array (Tennent 1967 a), this error is estimated to be of the order of 2° (in standard deviation) for showers, of typical sizes, in a near vertical cone.

If delays of subsequent particles are measured experimentally with respect to this first signal then the above theoretical distributions are changed considerably (Baxter *et al.* 1967). The delay in the first detected particle with respect to the true shower front results in a sharpening of the experimental distribution. (The maximum, containing many particles, does not suffer additional delay.) A comparison of the experimental and theoretical average first signal time-delay distributions is presented in figure 2 at 400 m and 600 m core distances.

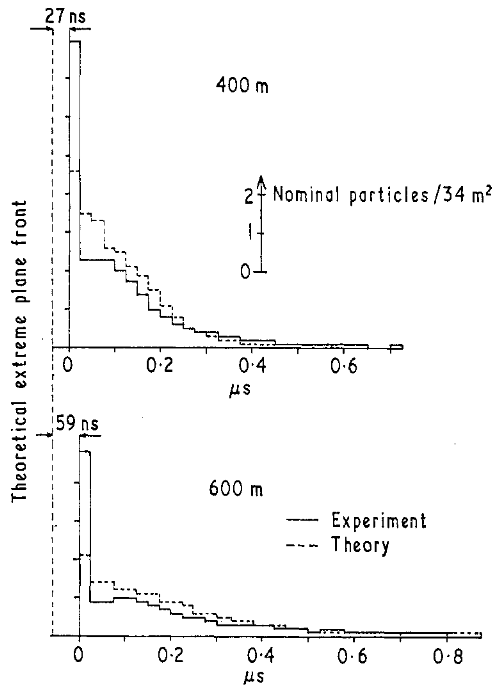


Figure 2. Comparison of the experimental and theoretical time delay distributions at 400 and 600 m.

A discrepancy between theory and experiment of the order of 50% still remains for the energy loss in the first 25 ns time interval. This may be partly explained if a less stringent criterion is employed as to what corresponds to the first detectable signal. If an observer of the experimental film record requires more than one muon to arrive before he can define a pulse origin (the single-muon level is just visible when isolated on a trace record), then there will be a greater apparent concentration of energy in the first time interval. Moreover, the calculations average the depths of the first few interaction points which may not be an appropriate approximation in this case.

The electron–photon time-delay distributions are less influenced by differences in the first few interactions, and are also subject to fewer sampling variations. Hence, they have been used to estimate the muon contribution to the experimental time distribution by aligning the late arrivals as presented in figure 3. A median height of production of the muon component can then be estimated, the steps leading to this being indicated in table 2.

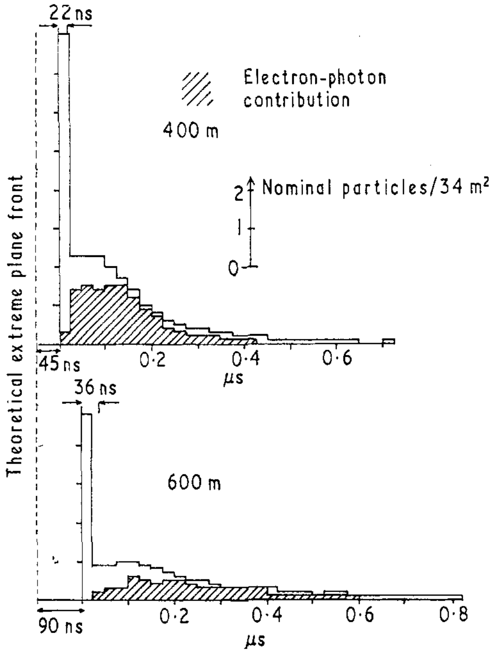


Figure 3. Estimated electron–photon contributions to the experimental time-delay distributions at 400 and 600 m.

**Table 2. An estimate of the median heights of muon production on subtraction of the electron–photon time-delay distribution from the experimental distribution**

| Core distance (m) | 400 | 600 |
|---|---|---|
| Plane front to first signal delay (ns) | $45 \pm 12$ | $90 \pm 40$ |
| Median muon delay with respect to plane front (ns) | $67^{+14}_{-12}$ | $126^{+66}_{-43}$ |
| Corresponding height of production (km) | $4{\cdot}0^{-0{\cdot}7}_{+0{\cdot}9}$ | $4{\cdot}7^{-1{\cdot}6}_{+2{\cdot}5}$ |
| Equivalent atmospheric depth (g cm$^{-2}$) | $650^{+50}_{-80}$ | $580^{+140}_{-170}$ |

These heights can be compared with a value of $320 \pm 70$ g cm$^{-2}$ derived by Linsley and Scarsi (1962), for almost the same size of shower. They are not regarded as inconsistent since their height has been averaged over a broad core distance range and is so biased in favour of larger distances; and also their array is at a higher elevation.

## 4. The energy flow

The computed integral photon energy spectrum at core distances of 200, 400 and 600 m is presented in figure 4. As the energies under consideration are almost all below the critical energy, photons are more numerous than electrons and the resultant electron energy spectrum is secondary to the photon spectrum. Also indicated is an experimental assessment due to Towers (private communication) of the spectrum at 450 m, the shape of which is in good agreement. The mean energy of the electromagnetic component per electron was found to remain nearly constant at 125 MeV over a core distance range of

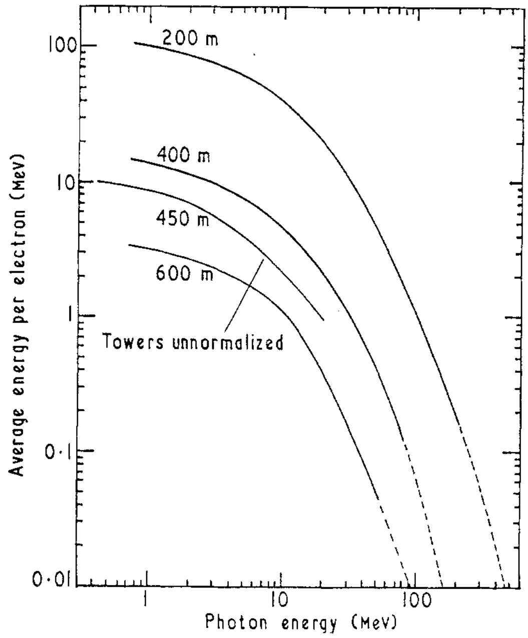


Figure 4. Integral photon energy spectra at core distances of 200, 400 and 600 m.

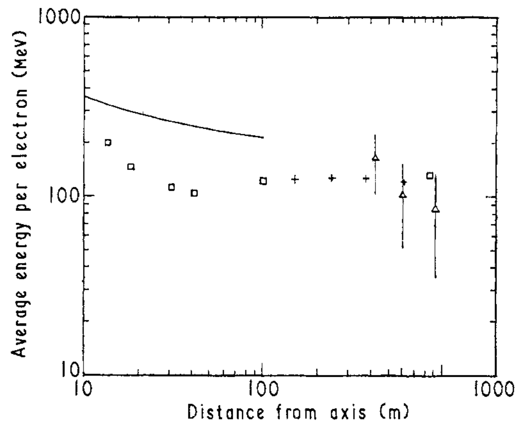


Figure 5. Lateral distribution of the average energy in the electron–photon component per electron.

150–800 m. This result, presented in figure 5, is a reasonable extrapolation to the results of Nishimura (1967) and Vernov *et al.* (1960) and is in good agreement with the results of Towers (private communication). Although the photon energy spectrum becomes softer with increasing core distance, the mean ratio of photons to electrons increases proportionately.

To define the shower structure in terms of particle numbers is difficult at low energies, both for the experimenter, who must resolve a particle in a detector of finite thickness, and for the theoretician, who must construct the possible electron paths. It is considered more profitable to express the cascade in terms of the total energy in the front, and to determine its absorption or energy loss in a 'deep' detector.

The predicted lateral distribution of energy in the electron–photon component at core distances 100–1000 m is shown in figure 6, together with an estimate of the electron numbers present. The Haverah Park array uses water Čerenkov detectors of depth 120 cm (Tennent 1967 b) which are nearly totally absorbing to photons at these energies. By

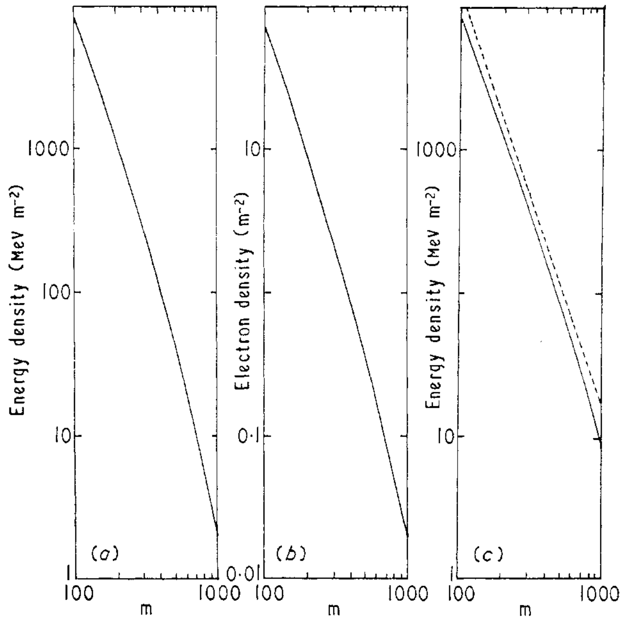


Figure 6. The predicted lateral distribution functions for a $9 \times 10^{16}$ ev shower: (*a*) energy in the electron–photon component; (*b*) electron number; (*c*) the total estimated energy loss of the electron–photon and muon components in the Haverah Park detectors. The broken line indicates an analytical power law energy loss, estimated from experimental results for this size of shower.

extending the calculation to predict the energy loss in such detectors, and including the estimated muon numbers present, as derived by Hillas (1966), one finds that the variation with core distance of the ratio between the muon contribution and the total detector response is as given in table 1. These ratios compare favourably with the ones determined experimentally for this size of shower (Allan *et al.* 1967). The lateral distribution of this total muon plus electron–photon detector energy loss is also shown in figure 6. In the experimental case this variation is approximated by an analytical power law relation:

$$D = (kN)r^{-n}$$

where $D$ is the energy loss density at a radial core distance $r$, $(kN)$ is a constant, a scaling factor appropriate to the primary energy of the shower in question, $n$ is termed the structure function exponent.

Such an approximation over the range 200–600 m indicates an exponent of 2·95 for the theoretical case which compares most favourably with a value of 2·90 (Suri 1966) for this size of shower in a near-vertical direction. Integrating the energy loss over the entire front at core distances 100–1000 m, a figure of $3{\cdot}90 \times 10^{14}$ ev is predicted for the electron–photon component and $1{\cdot}75 \times 10^{14}$ ev for the muon component. The total loss of $5{\cdot}65 \times 10^{14}$ ev corresponds to about 1/160th of the primary energy. This compares favourably, considering the nature of the calculation, with a value of 1/145 derived by Suri (1966) from a comparison of the Haverah Park shower rates with those presented in terms of primary energy by Greisen (1965).

**Acknowledgments**

The author is grateful for the opportunity of working at the S.R.C. Station for Cosmic Ray Shower Studies at Haverah Park, for facilities in the Leeds University Computing Laboratory and for a maintenance support grant from the Science Research Council.

He would particularly wish to thank Dr. A. M. Hillas for help and discussion, and for making available to him the results of (unpublished) calculations. He would also thank Professor J. G. Wilson and Dr. A. A. Watson for their interest and encouragement.

## Appendix 1. The modification of the Gaussian multiple-scattering distributions to include effective single-scattering events

According to Bethe's treatment (1953) of the Molière scattering theory, the probability $F(\theta)\mathrm{d}\theta$ that an electron will have been deflected through an angle $\theta$ and $\theta+\mathrm{d}\theta$ after traversing a distance $Z$ is given by

$$F(\theta)\,\mathrm{d}\theta = k\theta'\left\{f_0(\theta')+\frac{1}{B}f_1(\theta')+\,\dots\,+\frac{1}{B^n}f_n(\theta')\right\}\mathrm{d}\theta'.$$

Here $f_0(\theta')$ describes a Gaussian distribution in angle due to multiple scattering; the higher terms are corrections to this shape. The parameters $B$, $\theta'$ and $\chi_c$ are defined (for scattering in air) by the following equations:

$$B-\ln(B) = \ln(7170Z)$$

$$\chi_c^{\,2} = \frac{0{\cdot}6435Z}{E^2}$$

$$\theta' = \frac{\theta}{\chi_c B^{1/2}}$$

and $E$ is the effective energy (MeV) in the distance interval $Z$ (g cm$^{-2}$).

At small angles ($\theta' < 2$), Hanson *et al.* (1951) have shown that a better approximation to the zero-order term $f_0$ is obtained if $f_0$ is reduced by a factor $(1-1{\cdot}2/B)^{1/2}$. At very large angles, the first-order term approaches the single-scattering law $f_1(\theta') = 2\theta'^{-4}$ and, since higher-order terms decrease more rapidly, it is sufficient in the region ($\theta' > 2$) to represent the distribution $F(\theta)$ by these first two terms.

The probability of a large single-scattering event ($\theta' > 2$) relative to multiple scattering was estimated to be in the ratio ($0{\cdot}344/B$:1). If in the computations a single-scattering event was selected randomly, then the parameter $\theta'$ was obtained from a sampling of the $f_1$ term as tabulated numerically by Bethe (1953). For the multiple-scattering case, the lateral displacement and final orientation were derived from a random sampling of the relevant Gaussian expressions and scaled down at effective angles $\theta' < 2$.

## Appendix 2. The sampling of the shower front by a detector of finite area

Given the actual time-delay distribution in the shower front, a method is required to determine what a detector will record on average with respect to the first detectable signal.

For computing purposes it has been found that the easiest way to sample the actual front is to first express it in an integral form $T(N)$, which represents the absolute time $T$ at which $N$ particles will have arrived on average. The probability that two successive particles are separated by a time in which, on average, $x$ particles would have arrived is $\mathrm{e}^{-x}$. A random $x$ difference can be selected by solving

$$R = \mathrm{e}^{-x}$$

$$x = -\ln(R)$$

where $R$ is a random number in the range 0–1. The time $t_i$ at which the $i$th particle arrives with respect to the first signal is then

$$t_i = T(-\ln R_i - \ln R_{i-1} - \dots\ -\ln R_1) - T(-\ln R_1).$$

The sampling is terminated after the arrival of the $j$th particle when

$$-\ln R_{j+1} - \ln R_j - \dots - \ln R_1 > N_m$$

where $N_m$ is the average total number of particles expected. The distribution in values of $j$ for a series of samplings is Poissonian in form:

$$P_j(N_m) = \frac{\exp(-N_m)N_m{}^j}{j!}$$

so the method simulates generally the normal statistical fluctuations in the numbers detected.

## References


ALLAN, H. R., BLAKE, P. R., NEAT, K. P., and PIDCOCK, J. K., 1967, *Proc. Int. Conf. on Cosmic Rays, Calgary, Can. J. Phys.*, **46,** 98–101.

BASSI, P., CLARK, G., and ROSSI, B., 1953, *Phys. Rev.*, **92,** 441–51.

BAXTER, A. J., WATSON, A. A., and WILSON, J. G., 1966, *Proc. Int. Conf. on Cosmic Rays, London,* 1965, Vol. 2 (London: Institute of Physics and Physical Society), pp. 724–6.

BAXTER, A. J., WATSON, A. A., and WILSON, J. G., 1967, *Proc. Int. Conf. on Cosmic Rays, Calgary, Can. J. Phys.*, **46,** 9–12.

BETHE, H. A., 1953, *Phys. Rev.*, **89,** 1256–66.

BUTCHER, J. C., and MESSEL, H., 1960, *Nucl. Phys.*, **20,** 15–128.

GREISEN, K., 1966, *Proc. Int. Conf. on Cosmic Rays, London,* 1965, Vol. 2 (London: Institute of Physics and Physical Society), pp. 609–15.

HANSON, A. O., LANZL, L. H., LYMAN, E. M., and SCOTT, M. B., 1951, *Phys. Rev.*, **84,** 634–7.

HILLAS, A. M., 1966, *Proc. Int. Conf. on Cosmic Rays, London,* 1965, Vol. 2 (London: Institute of Physics and Physical Society), pp. 758–61.

LINSLEY, J., and SCARSI, L., 1962, *Phys. Rev.*, **128,** 2384–92.

LOCCI, M. A., PUICHI, P., and VERRI, G., 1967, *Nuovo Cim.*, **50B,** 384–8.

NISHIMURA, J., 1967, *Handb. Phys.*,**XLVI/2,** 1–114.

ROSSI, B., 1952, *High Energy Particles* (Englewood Cliffs, N.J.: Prentice-Hall).

SURI, A. N., 1966, *Ph.D. Thesis*, University of Leeds.

TENNENT, R. M., 1967 a, *Proc. Int. Conf. on Cosmic Rays, Calgary, Can. J. Phys.*, in the press.

—— 1967 b, *Proc. Phys. Soc.*, **92,** 622–31.

VERNOV, S. N., DMITRIEV, V. A., SOLOVIEVA, V. T., and KHRISTIANSEN, B. G., 1960, *Sov. Phys.-JETP.* **10,** 1050–1.